Aceh Int. J. Sci. Technol., 14(1) 63-73
April 2025
doi: 10.13170/aijst.14.1.44305

Aceh International Journal of Science and Technology
ISSN: p-2088-9860; e-2503-2398
Journal homepage: http://jurnal.usk.ac.id/aijst

Improved Performance on Inverted V Eccentrically Braced Frames (EBF) by Implementing Shear Link and Installing Web Stiffener in Link

Arief Panjaitan[1*], Purwandy Hasibuan[1], Rudiansyah Putra[1], Mochammad Afifuddin[1], Surya Bermansyah[1], Muttaqin Hasan[1], Muhammad Fauzi[1], Muhammad Haiqal[2], Muhammad Imran[3], Muhammad Fujii Hanafi[3], Masaru Shimizu[4]

[1]Civil Engineering Department, Faculty of Engineering, Syiah Kuala University, Banda Aceh, 23111, Indonesia;
[2]Architecture and Planning Department, Faculty of Engineering, Syiah Kuala University, Banda Aceh, 23111, Indonesia;
[3] Graduate School of Civil Engineering Department Alumni, Syiah Kuala University, Banda Aceh, 2311, Indonesia;
[4]Civil Engineering Department, Nagoya University, Furo-Cho, Chikusa-ku, Nagoya, 464-8614, Japan;

*Corresponding author: arief_panjaitan@usk.ac.id

Received : January 26, 2025
Received in revised from: April 28, 2025
Accepted : May 22, 2025
Online : June 4, 2025

Abstract – Eccentrically Braced Frame (EBF) is a structural system that is advised to be built in seismically active areas since they are characterized by good stiffness and ductility. A large and stable hysteretic curve, which corresponds to good seismic performance, is produced by the combination of improved stiffness and ductility in EBF. The diagonal component of EBF, known as a brace, contributes to its stiffness. Meanwhile, the short beam, also known as the link element, provides ductility in EBF. One element that is essential as an energy dissipator in EBF is a link element. By displaying a sizable and steady hysteretic curve, a prior study found that EBF with a flexural link could effectively dissipate the seismic energy. But to achieve a higher EBF, the seismic performance still needs to be enhanced. An analysis of various EBF models in Inverted V configurations was conducted in this paper. Each model was prepared with different shear link characteristics. Installing web stiffeners in the link to improve its seismic performance was also taken into consideration in this study. To obtain seismic performance, the cyclic loads were employed to each model under conditions of yield displacement control. Analysis of the data resulted in the load-displacement hysteretic curve. Next, using the hysteretic curve, the three seismic performance parameters, i.e., strength, stiffness, and dissipation energy were further developed. The investigation showed that compared to earlier studies, the EBF with shear links showed a bigger and more stable hysteretic curve which means better dissipated energy. Additionally, adding web stiffeners significantly increases the EBF's seismic capability. Therefore, because of the improved seismic characteristics, it is advised to establish the EBF using a shear link reinforced by web stiffeners in an earthquake-hazard area.

Keywords: Eccentrically Brace Frame (EBF), EBF configuration, link element, cyclic load, hysteretic loop, structural performance, dissipated energy

Introduction

The seismic-resistant structures have to be built in areas that are susceptible to earthquakes to ensure the building's strength. One seismic-resistant construction that combines strong stiffness and ductility to produce a large and stable hysteretic curve is the Eccentrically Braced Frame (EBF). Since its characteristics offer more space in the building than other EBF types, Inverted V EBF is typically used. Numerous studies have been carried out thus far to better understand EBF behavior and improve EBF seismic performance. Shi *et al.*, (2020) examined the seismic behavior of the semirigid-connection replaceable links in EBF and found that they had a better capacity for energy dissipation and superior inelastic rotation ability. An Eccentrically Braced Composite Frame (EBCF) that was updated with bending shear panel dampers (BSPDs) was also examined for seismic performance in a vertical direction (Zhuang *et al.*, 2020). In their evaluation of the advantages and effectiveness

doi: 10.13170/aijst.14.1.44305

of detachable links in EBF, Nastri and Plaitano (2022) revealed that when the links are combined with an elastic system, residual drift can be recovered. Mortazavi *et al*., (2020b) used steel casting technology to improve the ductility and low-cycle fatigue life of conventional EBF links. To increase the structural plasticity of EBF, Miao *et al*., (2022) looked into a new type of damper called a box damper, which is an enhanced type of shear panel damper. The prefabricated steel frame structure beam-column junction and EBF shapes were designed and studied in a former study (Sun *et al*., 2020). They presented the current state of the EBF structural system and a semi-rigid beam-column joint. Both component-level and system-level responses for steel EBF due to cyclic loading were also examined in previous research work (Azad & Topkaya, 2017). A nonlinear study, including the pushover analysis, which offers details on the collapse mechanisms and performance points, was also carried out (David and Sarif, 2020). The performance of EBF and Special Moment Resisting Frames (SMRF) was also compared in this study. Haris *et al*., (2020) investigated the relationship behavior of EBF with the varying link element and cross-sectional bracing with the ultimate load and ductility of the structure. Bahrami and Heidari (2020a) assessed the structural response of composite steel-concrete eccentrically Buckling-Restrained Braced Frames (BRBFs). An experimental investigation on the seismic performance of steel EBF with full bolt connections was done in a former study (Zhou *et al*., 2021). Bahrami and Heidari (2020b) provided the dynamic analysis of steel EBF with shear connections under various earthquake stresses, such as the Tabas, Chi-Chi, and Northridge earthquakes. Vinaykumar and Sunil (2020) carried out a comparative study of various load scenarios and load combinations in the V-EBF and V-CBF systems.

Using finite element software to evaluate steel EBFs with moment-shear links, Bahrami and Heidari (2020c) investigated the dynamic behavior of the EBFs. To improve the energy dissipation capacity, Yao *et al*., (2020) modified an Eccentrically Braced Lateral Force-Resisting System. The seismic performance of EBF made of high-strength steel with a vertical shear link was assessed in a previous study (Lian and Su, 2017). Under seismic pressure, (Mansour *et al*., 2011) examined two distinct types of replaceable links with varying section profiles, connection types, welding details, and intermediate stiffener spacings. (Fathali and Hoseini Vaez, 2020), who employed a novel approach for link beam modelling to assess its behavior investigated the idea of optimizing the EBF weight based on Performance Based Design (PBD). Rahnavard *et al*., (2017) presented EBF seismic behavior with single and double shear panels, in which the behavior of shear connections is assessed using numerical modeling using FE software under two types of cyclic displacement loads. Mortazavi *et al*.,(2024a) provided a summary of several studies that were conducted to enhance the functionality, construction, and design of EBFs. The impact of flexural link implementation in Inverted V EBF was analytically investigated in a former study and found that it can produce a big and stable hysteretic curve (Hanafi *et al*., 2024). Zhuang *et al*., (2020) examined the seismic performance of an eccentrically braced composite frame (EBCF) that was improved with bending shear panel dampers (BSPDs). The structural performance of multiple brace sections of Concentrically Brace Frame (CBF), i.e., single bracing (BR1), double bracing with batten plates (BR2), and double bracing with lacings (BR3) due to seismic activity, was also examined (Panjaitan *et al*., 2022). In their study of the seismic performance of various length double-section braces connected with batten plate (BP) and lacing (L), Panjaitan *et al*., (2023) discovered that shorter braces and L dissipate energy effectively by having a wider hysteretic curve.

Li *et al*., (2020) investigated the seismic behavior of replaceable shear link EBF with web opening and found that the frame's ultimate bearing capacity, initial stiffness, and energy consumption all showed a downward trend as the opening ratio increased. Jonathan *et al*., (2020) conducted a numerical analysis of the damage index in 2D steel buildings using EBF. Panjaitan *et al*., (2024a) experimentally examined several CBF braces under cyclic loads, with the braces being adjusted based on their sectional area. The seismic performance of many CBF models in Chevron V Brace and Diagonal configurations with varying frame heights was analytically examined by a former study (Panjaitan *et al*., 2023b). Panjaitan *et al*., (2024b) reported that the varied amplitude loading affected the single brace CBF's performance and found that the largest cumulative dissipated energy was attained in the same applied displacement by specimens loaded by the lesser number of cycles in a block amplitude.

The seismic behavior of steel seismic-resistant structures and EBF was covered in detail in several earlier studies. However, the link aspect must be upgraded to increase EBF's seismic capabilities. This aspect is installing the web stiffeners on the various spaces in the link. The seismic performance of the Inverted V EBF with a shear link was assessed in this study. Web stiffeners were installed to reinforce the link. The analysis was conducted to determine the contributions of the shear link to seismic capability and to observe the influence of stiffener strengthening in improving the EBF performance.

Aceh Int. J. Sci. Technol., 14(1) 63-73
April 2025
doi: 10.13170/aijst.14.1.44305

Materials and Methods

Three different FE models of the EBF are presented in this paper. As shown in Figure 1, they were constructed in an Inverted V arrangement. The shear link of each model was varied by the number of panels,

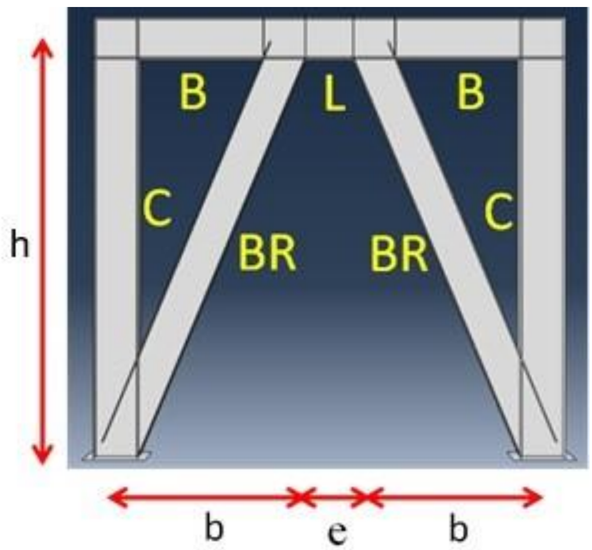

Where
- B : Beam
- C : Column
- BR : Brace
- L : Shear Link

EBF dimensions
- b = 4000 mm
- h = 1750 mm
- e = 500 mm

Figure 1. The configuration of Inverted V EBF and its components

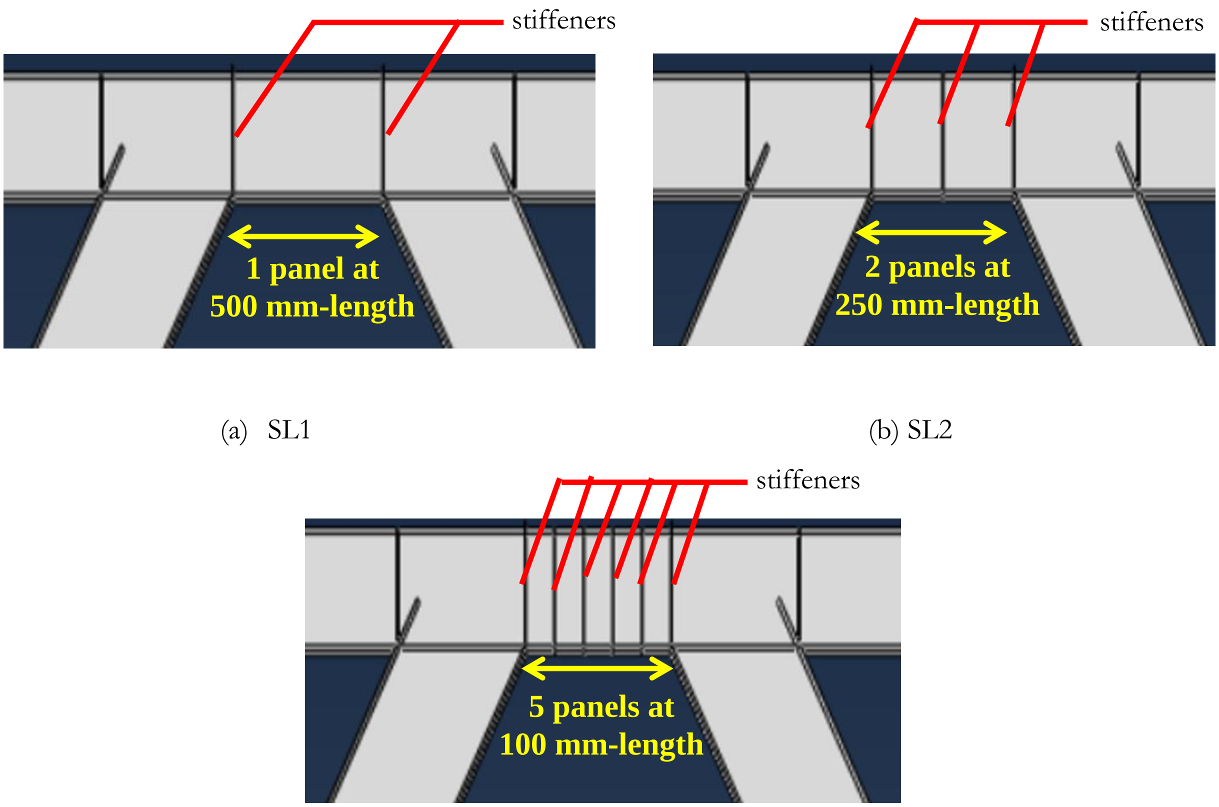

(a) SL1 (b) SL2

(c) SL3

Figure 2. Shear link models with different stiffener configurations (unit : mm)

Aceh Int. J. Sci. Technol., 14(1) 63-73
April 2025
doi: 10.13170/aijst.14.1.44305

Table 1. Profiles of CBF component

Notation`	Component	Section
B	Beam	IWF 400x300x16x10
C	Column	IWF 450x300x18x11
BR	Bracing	IWF 400x300x14x9
L	Link	IWF 400x300x16x10

Table 2. Characteristics of the Shear links-Inverted V EBF

Notation	Number of stiffeners on the link	Number of panels on the link	Length of a panel on the link (mm)
SL1	2	1	500
SL2	3	2	250
SL3	6	5	100

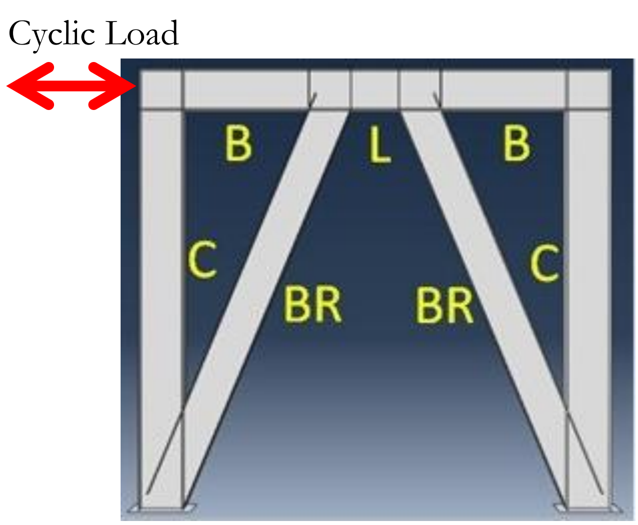

Figure 3. Implementation of cyclic loading

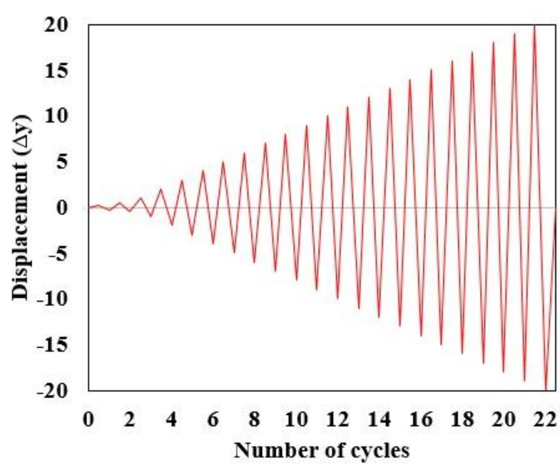

Figure 4. Loading protocol

i.e., SL1 (1 panel), SL2 (2 panels), and SL3 (5 panels), depending on the stiffener spaces. The installation of web stiffeners in various spaces is aimed at investigating the improved performance of EBF by adding the number of stiffeners in the link. Table 1 lists the component profiles. BJ 37 steel, which has a yield strength of 240 MPa and an ultimate strength of 370 MPa, was assigned to each component of EBF. In the modelling procedure, the material's kinematic hardening rule was determined after it reached the yield point. The yield surface is permitted to translate in the stress space during kinematic hardening, meaning that it maintains its size and shape while translating in the yielding direction. This analysis was conducted analytically using Abaqus FEA (Ver. 6.14), a finite element program. As shown in Figure 2, the cyclic load was applied in the frame's upper-left corner. Tensile-compressive axial forces were applied to the bracing as a result of the cyclic load.

Aceh Int. J. Sci. Technol., 14(1) 63-73
April 2025
doi: 10.13170/aijst.14.1.44305

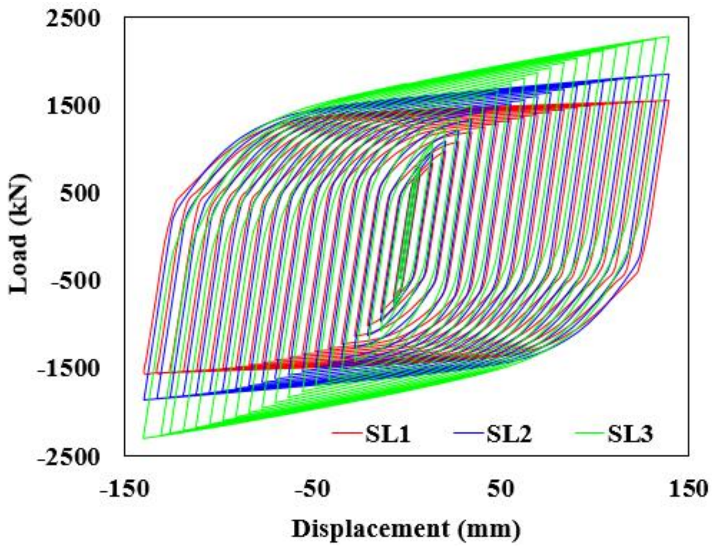

Figure 5. Load-displacement hysteretic curve of SL-EBF

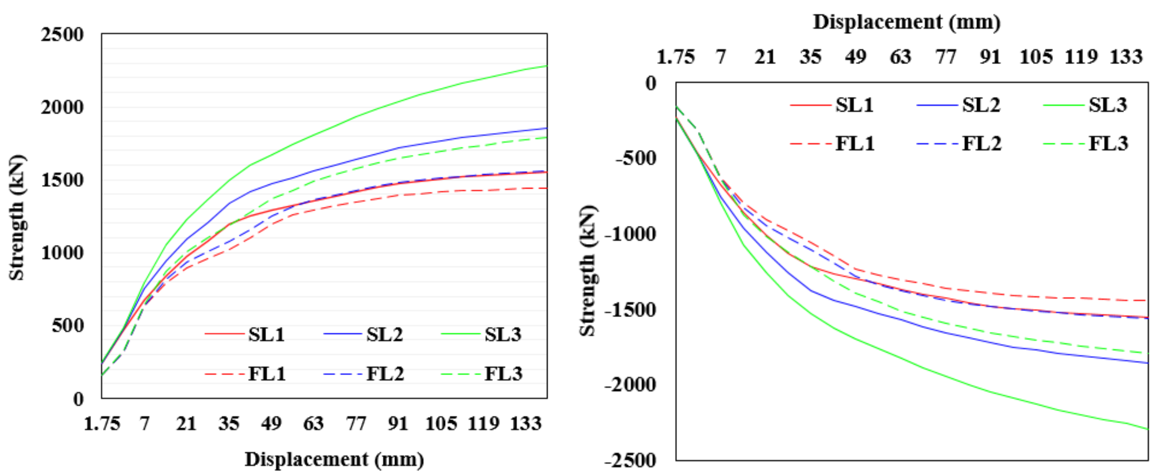

(a) Tension

(b) Compression

Figure 6. Strength

A schematic of cyclic loading with controlled yield displacement (δ_y) of the whole structural system is shown in Figure 3. To show the model behavior in the elastic range, the displacement control magnitudes in the first three cycles were set lower than the yield displacement, i.e., 0.25, 0.5, and 1.0 δ_y. Additionally, the models' elastic stiffness was obtained by using the elastic displacement controls. The models were simulated at the inelastic condition using an increasing rate of 1.0-yield displacement, or 1.0-yield displacement rate. The magnitude of 1-δ_y was 7.0 mm, and this value was obtained from pushover analysis. The model was subjected to 22 loading cycles (140 mm displacement) to obtain comprehensive results.

Aceh Int. J. Sci. Technol., 14(1) 63-73
April 2025
doi: 10.13170/aijst.14.1.44305

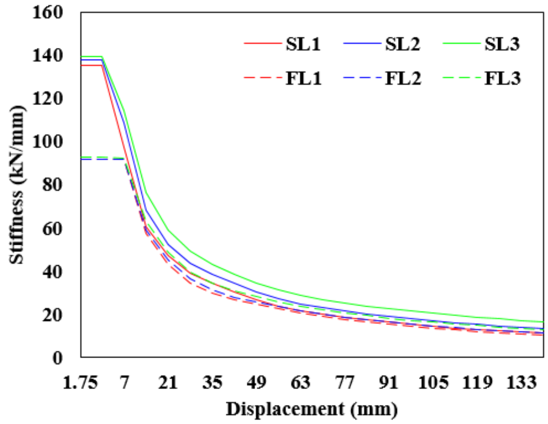

Figure 7. Stiffness

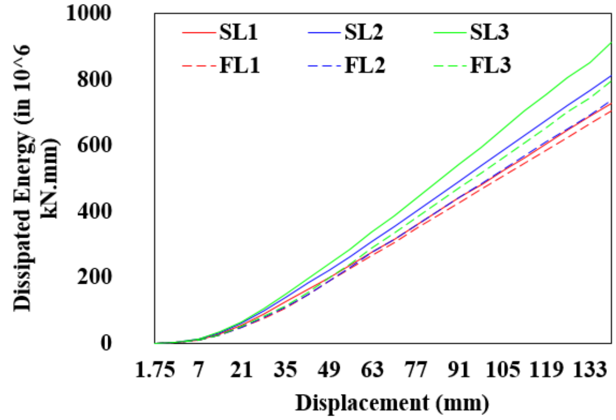

Figure 8. Dissipated Energy

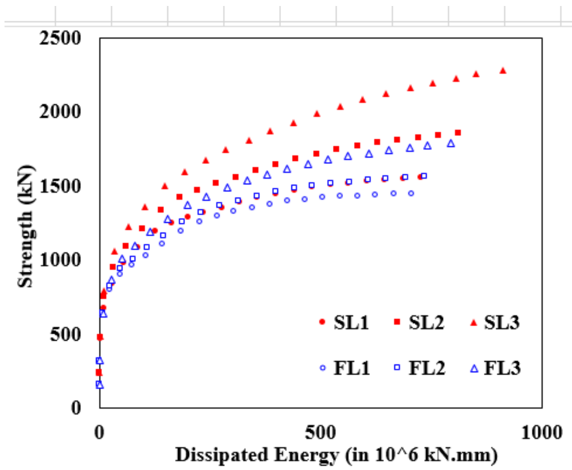

Figure 9. Strength - dissipated energy relationships

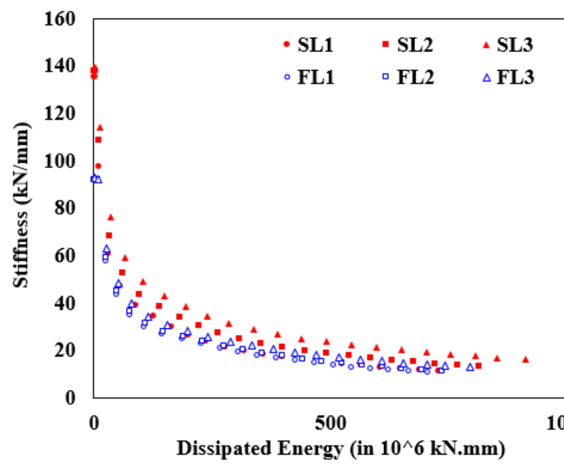

Figure 10. Stiffness - dissipated energy relationships

Results

The load-displacement hysteretic curve of an Inverted V Eccentrically Braced Frame (EBF) is shown in Figure 5. The figure demonstrates that in comparison to the SL1 and SL2, the EBF with a 100 mm stiffener space link (SL3) contributes the largest area of the hysteretic curve. This study is clarified with a previous investigation by (Hanafi *et al.*, 2023). Several Inverted V Eccentrically Brace Frames (EBF) with various 1000 mm length-flexural link (FL) configurations were investigated in this former study. These flexural links were link strengthened by stiffeners at both ends (FL1), link strengthened by stiffeners installed at 250 mm space (FL2), and link strengthened by stiffeners installed at 100 mm space (FL3).

Figure 6 illustrates the strengths of the EBF with shear link (SL) and EBF with flexural link (FL) for tension and compression. According to the figure, the EBF with shear link (SL) outperformed the EBF with flexural link (prior study) in terms of strength. For the shear link EBF (SL-EBF) and the flexural link EBF (FL-EBF), the greatest strength is determined in SL3 and FL3, respectively. The ultimate compressive strength (P_{uc}) of SL3 is 2289.73 kN, and the ultimate tensile strength (P_{ut}) is 2283.88 kN. The ultimate compressive strength (P_{uc}) of FL3 is 1793.76 kN, whereas the ultimate tensile strength (P_{ut}) is 1788.59 kN. The strength difference between the SL3 and SL1 would be 47% if those values were compared among SL-EBFs. Regarding the FL-EBF, the difference between FL3 and FL1 shows a strength disparity of 24%. Verification of SL3 and FL3 reveals that at the 22nd cycle (140 mm displacement), SL3's strength is 27.7% more than FL3's. With a ratio of 1.004, an analysis

doi: 10.13170/aijst.14.1.44305

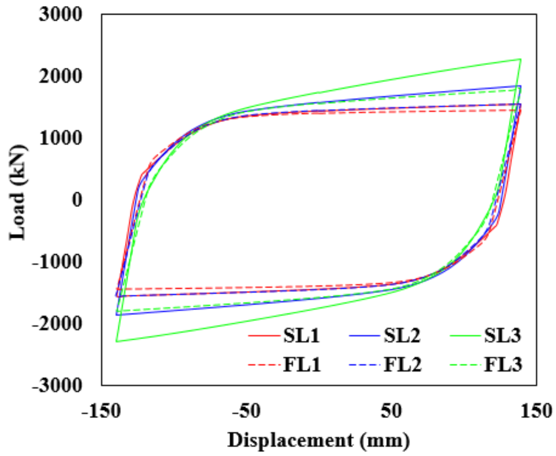

Figure 11. Envelope curves

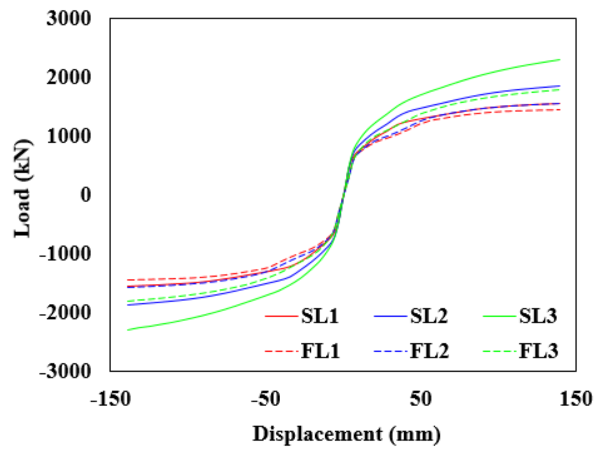

Figure 12. Backbone curves

of the strengths at the tensile and compressive regions showed that the compression strengths were slightly greater than the tension strengths, indicating that the Bauschinger effect from cyclic loading was negligible.

Figure 7 shows the stiffness of the EBF models for each cycle. The SL-EBF is stiffer than the FL-EBF (former study), as the figure illustrates. Out of all the SL-EBFs, the SL3 is the stiffest, and out of all the FL-EBFs, the FL3 is the stiffest. Additionally, the figure demonstrates that for all EBFs, the stiffness values expressed in the first three cycles are constant. To identify the stiffness at the elastic state, those cycles were applied with values below 1-δ_y, as previously explained. The SL3 has a stiffness (K) of 16.38 kN/mm, with the highest inelastic stiffness indicated at the 22nd cycle. The stiffness of the FL3 is 12.84 kN/mm. There is a 47.04% stiffness difference between SL3 and SL1, according to verification. A stiffness gap of 24.04% is identified when the FL3 to FL1 is clarified. Furthermore, at the 22nd cycle, the SL3's stiffness is 26.64% higher than the FL3's, indicating that the SL3 is stiffer than the FL3. Additionally, Figure 7 demonstrates that as loading cycles continue, the stiffness decreases, suggesting that the link components' yield has spread. The EBF strength only marginally increases with cycle sustenance because of the yield condition.

The dissipated energy for the FL EBF and SL-EBF is shown in Figure 8. The cumulative energy magnitudes for the first three cycles are not shown. At these cycles, there are no regions of the load-displacement curve that match the zero-dissipated energy because of the elastic condition. The SL3 provides higher dissipated energy (E_d SL3) than the SL1 (E_d SL1) and SL2 (E_d SL2), according to an observation made at the 22nd cycle. It is also observed that FL3 (E_d FL3) has a higher dissipated energy than FL1 (E_d FL1) and FL2 (E_d FL2). It is also figured out that the SL-EBFs have higher dissipated energy compared to FL-EBFs.

Figure 9 shows the relationships between strength and dissipated energy. According to the figure, the strength plots exhibit a sharply growing tendency at lower dissipated energy values, and they tend to exhibit little upward trends as the dissipated energy escalation continues. This behavior is characterized for all models. Verifying the SL-EBF against the FL-EBF shows that the SL-EBF improves seismic performance in terms of strength and energy dissipation. Furthermore, the strength and dissipated energy were significantly increased by installing the web stiffeners and positioning them in narrower spaces, i.e., SL3 has higher stiffness and dissipated energy than SL1 and SL2. Similar patterns were also discovered in FL-EBF, where the FL3 performs the better stiffness and dissipated energy that those showed by FL1 and FL2.

The stiffness and dissipated energy relationships are depicted in Figure 10. According to the figure, as the additional values of dissipated energy increased, the stiffness decreased. At low dissipated energy levels, the stiffness was much reduced, and then the stiffness reduction led to being more gentle at the sustenance of dissipated energy. This trend is equally observed in all EBF models. In comparison to the FL-EBF, the SL-EBF also contributed to greater stiffness and dissipated energy. Verifying the influence of installing web stiffeners and reducing the distance between two stiffeners (panels), it is shown that both strengthening techniques increase

doi: 10.13170/aijst.14.1.44305

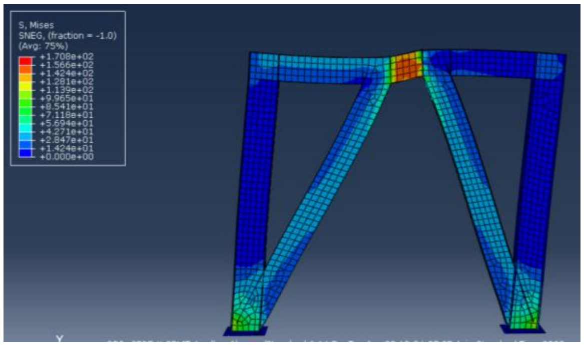

(a) 2nd displacement cycle (0.5 δ_y)

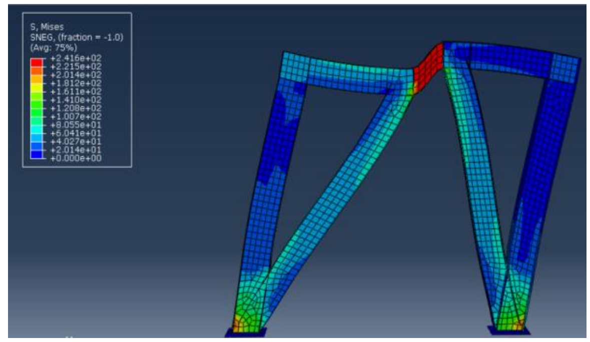

(b) 3rd displacement cycle (1.0 δ_y)

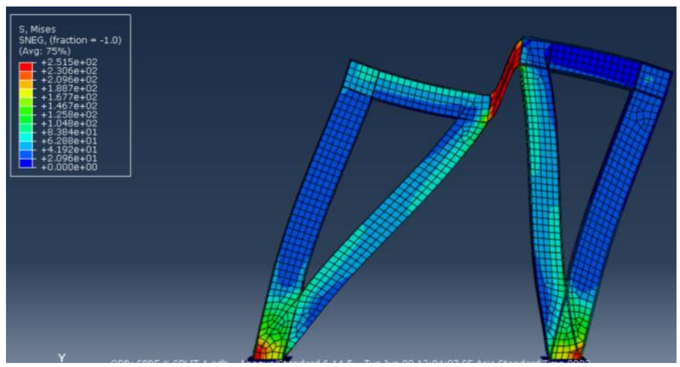

(c) 4th displacement cycle (1.5 δ_y)

Figure 13. Equivalent stress (Von Mises stress) distribution in SL1-EBF

EBF stiffness, i.e., the SL3 achieved a higher stiffness than SL1 and SL2. In FL-EBF, the comparable tendencies were also indicated. The stiffness of the FL3 was higher than that of the FL1 and FL2.

In order to acquire the largest hysteretic area that attributes to the envelope conditions, envelope curves are given by displaying the load-displacement hysteretic curve at the final loading application cycle. The envelope curves that originated from SL-EBF and FL-EBF were shown in Figure 11. Regardless of installation and uninstallation of the web stiffeners, the figure indicates that SL-EBFs perform larger envelopes than FL-EBFs. Additionally, the envelope area, which is observed in SL-EBF and FL-EBF, is increased by installing stiffeners in the link and positioning them in smaller gaps.

Plotting displacement and load from elastic to plastic conditions illustrates backbone curves as shown in Figure 12. The figure shows the tendencies of the SL-EBF and FL-EBF backbone curves. At the elastic condition, load-displacement relationship tends to be linear. At the plastic conditions, both displacement and load were plotted in their yield and ultimate point in each cycle and performs non-linearity in load-displacement curves. Figure 12 also illustrates that SL-EBF specifies stiffnesses that are higher than FL-EBF's. The steeper slope of the load-displacement backbone curves in SL-EBFs addressed to the greater stiffnesses. In comparison to EBFs without web stiffeners, SL-EBF and FL-EBF exhibit significantly higher stiffness when web stiffeners are installed and web panels are managed in narrow gaps.

Discussion

The link is an energy dissipator in EBF. Accordingly, to enhance the seismic performance of EBF, the link was connected to the EBF beam by using the end-plate connection. In previous research work, two EBF specimens were prepared in the laboratory. The first EBF was specified by using a link with a combination of bolted and welded connections in its end plate. The second EBF was designed by implementing a link with welded connections in the end plate. The result discovered that utilizing a fully welded connection at the end plate of the link component results in better seismic performance in EBF (Moestopo *et al.*, 2012). Panjaitan *et al.*, (2024c) investigated the flexural strength of several end-plate connections, and this connection type has been widely used to join beam-link elements. The study revealed that flexural strength linearly escalated with the additional length of the bolted connection.

Compared to the former study (Hanafi *et al.*, 2023), this present study, which implements SL-EBF, demonstrates a higher strength than that of previous research work (FL-EBF) as shown in Figure 6. This behavior is highly expected since the shorter links in SL-EBF produce smaller internal moments than those of longer links in FL-EBF. The smaller internal moments will result in higher strength in SL-EBF. The stiffness trends of FL-EBF and SL-EBF are shown in Figure 7. The figure depicts that the stiffness leads to show degradation trend together with additional values of displacement. This behavior is caused by the link element's yield conditions, where the yield spreads as the cyclic displacement continues. Since the SL-EBF is stronger than the FL-EBF at the same applied displacement, it also exhibits more stiffness than the FL-EBF.

The dissipated energy is shown in Figure 8. Since the yield extension mechanism occurs in the link area, the dissipated energy increases exponentially with additional displacement values, as shown in the figure. The installation of web stiffeners was also shown to be important in enhancing the strength, stiffness, and dissipated energy in SL-EBF and FL-EBF, as illustrated in Figures 9 and 10. Installing web stiffeners will first enhance the stiffness of the link and then improve the strength and dissipated energy of EBF. The envelope curves of SL-EBF and FL-EBF are shown in Figure 11. The figure shows that the SL-EBF contributes a larger envelope than the FL-EBF, indicating that the SL-EBF has a better yield spreading mechanism. In Figure 12, the backbone curve is displayed. From the figure, a stiffer EBF was specified in SL-EBF than the FL-EBF. This behavior is figured out since the SL-EBF has a shorter link than the FL-EBF. The shorter link is highly expected to be difficult to experience the flexural deformation and result in stiffer characteristics in SL-EBF. Figure 13, which corresponds to SL1-EBF, shows the yield spreading in the link element as a result of the yield extension mechanism. The observations were emphasized in the 2nd, 3rd, and 4th of cyclic displacements. From the figure, it is noticed that the yield area is extensively spread from the small to the large area during the sustenance of cyclic loading. This figure also analytically indicated that the link element is a seismic energy dissipator in EBF due to higher equivalent stress, which is calculated in this component.

Conclusion

This research analytically investigated the performance of Inverted V Brace EBF by considering the shear link as its energy dissipator. There were three types of shear links, i.e., link without stiffener (SL1), link with 250 mm-stiffener space (SL2), and link with 100 mm-stiffener space (SL3). The present study was then verified to the former study. The previous study analyzed the flexural link in EBF, i.e., link without stiffener (FL1), link with 250 mm-stiffener space (FL2), and link with 100 mm-stiffener space (FL3). Observing seismic performance in SL-EBF and FL-EBF which are composed of strength, stiffness, and dissipated energy revealed that the SL-EBF is better than FL-EBF. The better seismic performance was supposedly present since the SL-EBF which has a shorter link than FL-EBF led to higher strength. Namely, due to the higher strength, the stiffness and dissipated energy also escalated. Examining the installation of the web stiffeners and configuring the stiffener on the narrower spaces disclosed that both strengthening approaches considerably improved the seismic capability of EBF. Furthermore, a better envelope curve that corresponds to better-dissipated energy and a better backbone curve was presented by SL-EBF and also by the EBF strengthened by the web-stiffeners in its link. As per the research investigations, better seismic capabilities were contributed by SL-EBF with a link reinforced by the web stiffeners. Accordingly, it is recommended to establish SL-EBF with web stiffeners to result in stronger construction, particularly in the area that is prone to earthquakes.

References

Azad, S.K. and Topkaya, C. 2017. A Review of Research on Steel Eccentrically Braced Frames. *Journal of Constructional Steel Research*, 128(4): 53-73. http://dx.doi.org/10.1016/j.jcsr.2016.07.032

Bahrami, A. and Heidari, M. 2020. Dynamic Analysis of Steel Eccentrically Braced Frames with Shear Link. *International Journal of Engineering Research and Technology*, 13(2): 233-239. http://dx.doi.org/10.37624/IJERT/13.2.2020.233-239

Bahrami, A. and Heidari, M. 2020. Dynamic Behaviour of Steel Eccentrically Braced Frames Having Moment-Shear Link. *ARPN Journal of Engineering and Applied Sciences,* 15(23): 2793-2799. https://www.arpnjournals.org/jeas/research_papers/rp_2020/jeas_1220_8419.pdf

Bahrami, A. and Heidari, M. 2020. Evaluation of Structural Response of Composite Steel-concrete Eccentrically Buckling-restrained Braced Frames. *Journal of Applied Engineering Science*, 18(4): 591–600. http://dx.doi.org/10.5937/jaes0-25497

David, R.G., and Sarif, N. 2020. Seismic Performance of Eccentrically Braced Frames. *IOP Conference Series: Materials Science and Engineering*, 989(1): 1-9. http://dx.doi.org/10.1088/1757-899X/989/1/012021

Fathali, M.A. and Hoseini Vaez, S.R. 2020. Optimum Performance-based Design of Eccentrically Braced Frames. *Engineering Structures*, 202: 1-15. http://dx.doi.org/10.1016/j.engstruct.2019.109857

Hanafi, M.F., Hasan, M., Panjaitan, A. and Shimizu, M. 2024. Seismic Performance of IWF Flexural Link in Inverted-V Eccentrically Braced Frames with Different Stiffener Spaces. *E3S Web of Conferences*, 476: 1-9. https://doi.org/10.1051/e3sconf/202447601009

Haris, S., Nidiasari and Putri, S.T.P. 2020. Numerical Study of Bracing Section Variations in an Eccentrically Braced Frame. *E3S Web of Conferences*, 156: 1-7. https://doi.org/10.1051/e3sconf/202015605012

Jonathan, V., Orientilize, M. and Sentosa, B.O.B. 2020. Numerical Study of Damage Index of 2D Steel Building with Eccentrically Braced Frame Using Opensees. *IOP Conference Series: Materials Science and Engineering*, 801(1): 1-9. http://dx.doi.org/10.1088/1757-899X/801/1/012022

Li, T., Shi, Q., Wang, X. and Ye, C. 2020. Study on The Seismic Behavior of Eccentrically Braced Steel Frames of Replaceable Shear Links with Web Opening. *Journal of Physics: Conference Series*, 1637(1): 1-8. http://dx.doi.org/10.1088/1742-6596/1637/1/012036

Lian, M. and Su, M. 2017. Seismic Performance of High-strength Steel Fabricated Eccentrically Braced Frame with Vertical Shear Link. *Journal of Constructional Steel Research*, 137: 262–285. https://doi.org/10.1016/j.jcsr.2017.06.022

Mansour, N., Christopoulos, C. and Tremblay, R. 2011. Experimental Validation of Replaceable Shear Links for Eccentrically Braced Steel Frames. *Journal of Structural Engineering*, 137(10): 1141–1152. http://dx.doi.org/10.1061/(ASCE)ST.1943-541X.0000350

Miao, F., Nejati, F., Zubair, S.A.M. and Yassin, M.E. 2022. Seismic Performance of Eccentrical Braced Frame Retrofitted by Box Damper in Vertical Links. *Buildings*, 12(10): 1-21. https://doi.org/10.3390/buildings12101506

Moestopo, M., Novan, A., Mirza, A., Pandjaitan, A.R. and Utomo, W.Y. 2012. On Improved Performance of Eccentrically Braced Frames with Replaceable Shear Link. The 15th World Conference on Earthquake Engineering, Lisboa, Portugal: 1-6. https://www.iitk.ac.in/nicee/wcee/article/WCEE2012_5803.pdf

Mortazavi, P., Kwon, O.S. and Christopoulos, C. 2024. Recent Advancements in Design and Fabrication of Eccentrically Braced Frames for Enhanced Ductility, Stability, and Resilience. 18th U.S.-Japan-New Zealand Workshop on The Improvement of Structural Engineering and Resilience, 1-9.

Mortazavi, P., Lee, E., Binder, J., Gray, M., Kwon, O. and Christopoulos, C. 2020. Overview of Experimental Program on Cast-steel Replaceable Yielding Links in Eccentrically Braced Frames. 17th World Conference on Earthquake Engineering, 17WCE, Sendai, Japan, September 13 to 18 2020: 1-13.

Nastri, E. and Plaitano, F. 2022. A Review on The Removable Link in Eccentrically Braced Frames: benefits and performances. *AIP Conference Proceedings*, 2425: 1-4. http://dx.doi.org/10.1063/5.0081521

Panjaitan, A., Hasibuan, P. and Haiqal, M. 2022. Kajian Kinerja Struktural Elemen Bresing SRBK dengan Tipe Penampang Tunggal dan Ganda Terhadap Beban Siklik. *Jurnal Arsip Rekayasa Sipil dan Perencanaan*, 5(4): 257–264. http://dx.doi.org/10.24815/jarsp.v5i4.28271

Panjaitan, A., Hasibuan, P., Putra, R., Afifuddin, M., Bermansyah, S. and Haiqal, M. 2024. Structural Performance of Single and Double-section CBF Braces with Different Lengths Under Cyclic Loading. *E3S Web of Conferences*, 476: 1-10. https://doi.org/10.1051/e3sconf/202447601003

Panjaitan, A., Hasibuan, P., Putra, R., Afifuddin, M., Fauzi, M. and Haiqal, M. 2024. Flexural Strength of End-plate Connection with Several Different Bolt Arrangements. *Journal of Physics: Conference Series*, 2916(1): 1-11. https://doi:10.1088/1742-6596/2916/1/012019

Panjaitan, A., Hasibuan, P., Putra, R., Afifuddin, M. and Haiqal, M. 2024. Seismic Performance of CBF's Single Steel Angle Brace Under Several Variable Amplitude Loadings. *Journal of Physics: Conference Series*, 2916(1): 1-11. https://doi.org/10.1088/1742-6596/2916/1/012003

Panjaitan, A., Hasibuan, P., Putra, R., Afifuddin, M. and Haiqal, M. 2023. Kinerja Bresing SRBK dengan Variabel Panjang Batang yang Berbeda Terhadap Beban Siklik. *Jurnal Teknik Sipil Universitas Syiah Kuala*, 12(1): 34-41. https://jurnal.usk.ac.id/JTS/article/view/31388/18022

Panjaitan, A., Hasibuan, P., Putra, R., Afifuddin, M., Haiqal, M., Adian, F., Naulia, D.P. and Hazid, A. 2023. The Performance of Concentrically Braced Frames (CBF) in Chevron V Brace and Diagonal Configuration by Considering Various Frame Heights. *Aceh International Journal of Science and Technology*, 12(2): 139–147. https://doi.org/10.13170/aijst.12.2.30848

Rahnavard, R., Hassanipour, A., Suleiman, M. and Mokhtari, A. 2017. Evaluation on Eccentrically Braced Frame with Single and Double Shear Panels. *Journal of Building Engineering*, 10: 13–25. https://doi.org/10.1016/j.jobe.2017.01.006

Shi, Q., Yan, S., Wang, X., Sun, H. and Zhao, Y. 2020. Seismic Behavior of The Removable Links in Eccentrically Braced Frames with Semirigid Connections. *Advances in Civil Engineering*, 2020(2): 1-26. http://dx.doi.org/10.1155/2020/9405107

Sun, H., Shi, Q., Wang, X., Li, T. and Zhangshuo, Z. 2020. A Review of Research on Seismic Performance of Steel Eccentrically Braced Frames in Prefabricated Buildings. *IOP Conference Series: Earth and Environmental Science*, 455(1): 1-9. http://dx.doi.org/10.1088/1755-1315/455/1/012066

Vinaykumar H.K. and Sunil, R. 2020. Comparative Study of Concentrically V Braced System and Eccentrically V Braced System for Steel Building. *International Research Journal of Engineering and Technology*, 7(10): 595-601. https://www.irjet.net/archives/V7/i10/IRJET-V7I10100.pdf

Yao, Z., Wang, W., Fang, C. and Zhang, Z. 2020. An Experimental Study on Eccentrically Braced Beam-through Steel Frames with Replaceable Shear Links. *Engineering Structures*, 206: 1-16. https://doi.org/10.1016/j.engstruct.2020.110185

Zhou, X., Wang, X., Yu, Y., Li, T. and Shi, Q. 2021. Experimental Study on Seismic Performance of Eccentrically Braced Steel Frame with Full Bolts Connection. *IOP Conference Series: Earth and Environmental Science*, 719(2): 1-8. http://dx.doi.org/10.1088/1755-1315/719/2/022051

Zhuang, L., Huang, D. and Chen, H. 2020. Seismic performance of eccentrically braced composite frame with bent shear panel dampers. 17 th World Conference on Earthquake Engineering, 17WCEE Sendai, Japan - Sept13th to 18th, 1-12.